Bromocarbons in the tropical coastal and open ocean atmosphere during the 2009 Prime Expedition Scientific Cruise (PESC-09)

Mohd Shahrul Mohd Nadzir[a,b,c,*], Siew Moi Phang[c], Mhd Radzi Abas[a,c], Noorsaadah Abd. Rahman[a,c], Azizan Abu Samah[b,c], , William T. Sturges[d], David E. Oram[d,g], Graham P. Mills[d], Emma C. Leedham[d], J. A. Pyle[e,g], N. R. P. Harris[e], A. D. Robinson[e], M. J. Ashfold[e,**], M.I. Mead[e,***], Mohd Talib Latif[h,i] , Md. Firoz Khan[h], and Abd Muhaimin Amiruddin[f]

[a] Environmental Research Group, Department of Chemistry, University Malaya, 50603 Kuala Lumpur

[b] National Antarctic Research Centre, IPS Building, University Malaya, 50603 Kuala Lumpur. Malaysia.

[c] Institute of Ocean & Earth Sciences, C308 IPS Building, University Malaya, 50603 Kuala Lumpur. Malaysia.

[d] Centre for Ocean and Atmospheric Sciences, School of Environmental Sciences, University of East Anglia, Norwich, NR4 7TJ, UK

[e] Centre for Atmospheric Science, Department of Chemistry, University of Cambridge, Lensfield Road, Cambridge, CB2 1EW.

[f] Department of Environmental Management, Faculty of Environmental Studies. Universiti Putra Malaysia., 43400 Serdang, Selangor. Malaysia

[g] National Centre for Atmospheric Science, UK

[h] Research Centre for Tropical Climate Change System (IKLIM) , Faculty of Science and Technology, Universiti Kebangsaan Malaysia.

[i] School of Environmental and Natural Resource Sciences, Faculty of Science and Technology, Universiti Kebangsaan Malaysia.

[*] now at: School of Environmental and Natural Resource Sciences, Faculty of Science and Technology, Universiti Kebangsaan Malaysia.

[**] now at: School of Biosciences, University of Nottingham Malaysia Campus, Jalan Broga, 43500 Semenyih, Selangor Darul Ehsan, Malaysia.

[***] Now at: Institute of Ocean & Earth Sciences, C308 IPS Building, University Malaya, 50603 Kuala Lumpur. Malaysia.

Keywords: VSLS bromocarbons; seaweed; chlorophyll-*a*; satellite measurements.

* Tel.: +60-389213861; fax: +60-389253357

E-mail address: shahrulnadzir@ukm.my

Abstract

Atmospheric concentrations of very short-lived species (VSLS) bromocarbons, including $CHBr_3$, CH_2Br_2, $CHCl_2Br$, $CHClBr_2$, CH_2BrCl, were measured in the Strait of Malacca, the South China and Sulu-Sulawesi Seas during a two month research cruise in June-July 2009. The highest bromocarbon concentrations were found in the Strait of Malacca, with smaller enhancements in coastal regions of Northern Borneo. $CHBr_3$ was the most abundant bromocarbon, ranging from 5.2 pmol mol^{-1} in the Strait of Malacca to 0.94 pmol mol^{-1} over the open ocean. Other bromocarbons showed lower concentrations, in the range of 0.8-1.3 pmol mol^{-1} for CH_2Br_2, 0.1-0.5 pmol mol^{-1} for$CHCl_2Br$ and 0.1-0.4 pmol mol^{-1} for $CHClBr_2$. There was no significant correlation between bromocarbons and *in situ* chlorophyll-*a* but positive correlations with both MODIS and SeaWiFS satellite's chlorophyll-*a*. Together the short-lived bromocarbons contribute an average of 8.9 pmol mol^{-1} (range 5.2-21.4 pmol mol^{-1}) to tropospheric bromine loading, which is similar to that found in previous studies from global sampling networks (Montzka et al., 2011). Statistical tests showed strong Spearman correlations amongst brominated compounds, suggesting a common source. Log-log plots of $CHBr_3/CH_2Br_2$ versus $CHBr_2Cl/CH_2Br_2$ show that both chemical reactions and dilution into the background atmosphere contribute to the composition of these halocarbons at each sampling point. We have used the correlation to make a crude estimate of the regional emissions of $CHBr_3$ and derive a value of 32 Gg yr^{-1} for the South East (SE) Asian region (10°N-20°S, 90°E-150°E). Finally, we note that satellite-derived chlorophyll-*a* (chl-*a*) products do not always agree well with *in situ* measurements, particularly in coastal regions

of high turbidity, meaning that satellite chl-*a* may not always be a good proxy for marine productivity.

1 Introduction

In recent years there has been a growing interest in the role of short-lived halocarbons in atmospheric chemistry, in particular their potential involvement in stratospheric ozone depletion. The term very short-lived substances (VSLS) has been used to represent halogen-containing compounds with lifetimes less than six months (WMO, 2007). Bromine-containing VSLS and their atmospheric degradation products are believed to account for around a quarter of total bromine entering the lower stratosphere (Dorf et al., 2006; Salawich et al., 2006; Montzka et al., 2011) and contribute to the 'missing' bromine (6 pmol mol^{-1}, range 3-8 pmol mol^{-1}) required to the levels of inorganic bromine Br_y and BrO measured in the stratosphere (Montzka et al., 2011).

The main brominated VSLS identified to date include bromoform ($CHBr_3$), dibromomethane (CH_2Br_2), dichlorobromomethane ($CHCl_2Br$), dibromochloromethane ($CHClBr_2$) and bromochloromethane (CH_2BrCl). Biogenic emissions from the oceans have been identified as one of the main natural sources, where organisms such as macroalgae (seaweeds) and microalgae (phytoplankton) can release large quantities of halocarbon gases to the atmosphere (Sturges et al., 1993; Moore et al., 1996; Laturnus and Adams, 1998). Previous ship and coastal measurements have collected bromocarbon data for many different global regions, summarised in Montzka et al. (2011). These studies show large temporal and spatial variability in both seawater and atmospheric concentrations, emphasizing the importance of localised emissions of these gases.

Because of their short atmospheric lifetimes, the region where VSLS are emitted into the atmosphere is significant and their O_3 depletion potentials (ODPs) vary accordingly (Ko et al., 2003). Tropical regions are believed to be the most important location for rapid transport of air from the surface to the upper troposphere and lower stratosphere. In the tropics, deep convection provides a major pathway for rapid transport of insoluble gases from the lower to the upper troposphere. Importantly, such convective transport appears to be particularly strong over the western Pacific (Gettelman et al., 2002; Fueglistaler et al., 2004). Furthermore, the warm, shallow waters of the tropical warm pool make them potentially important source regions for biologically-produced halocarbons. Therefore, this region has the potential to supply a proportion of the 'missing' ~6 pmol mol^{-1} of bromine, thought to be related to VSLS, to the stratosphere.

Yokouchi et al. (1997) were the first to report atmospheric bromocarbon measurements in the Strait of Malacca and the South China Sea. During a cruise between Japan and the Bay of Bengal they measured mean concentrations of 0.77 pmol mol^{-1} (max 1.42 pmol mol^{-1}) and 1.2 pmol mol^{-1} (max 7.1 pmol mol^{-1}) for CH_2Br_2 and $CHBr_3$, respectively. The highest levels were seen in harbour regions of Singapore and Penang and the authors suggested a link between high $CHBr_3$ concentrations and high chlorophyll-*a* (chl-*a*) and the influence of algal sources. During a cruise in the South China Sea, Quack and Suess (1999) observed mean ambient air concentrations for bromoform of 1.2 pmol mol^{-1} (range 0.38-10.67 pmol mol^{-1}).

A second cruise reported in Yokouchi et al. (1997) was made in the western Pacific (Japan-SE Australia) where atmospheric mixing ratios were observed in the range of 0.13-2.9 pmol mol^{-1} for $CHBr_3$ and 0.14-1.58 pmol mol^{-1} for CH_2Br_2. More recently, Yokouchi et al. (2005) reported a larger range of bromocarbon concentrations, with $CHBr_3$ ranging from

~1 pmol mol^{-1} over the open ocean to ~40 pmol mol^{-1} in the vicinity of tropical islands in the western Pacific region. Butler et al. (2007a) collected data from seven open ocean cruises spanning a ten-year period, covering much of the world's oceans. Their tropical air mean mixing ratios for $CHBr_3$ and CH_2Br_2 were 1 pmol mol^{-1} (0.4-2.1 pmol mol^{-1}) and 0.9 pmol mol^{-1} (0.6-1.3 pmol mol^{-1}) respectively.

Despite these measurements collected over the last two decades, the seas and coastlines of SE Asia are still vastly under-represented. This knowledge gap introduces uncertainties in our understanding of the global distributions and fluxes of bromocarbons and therefore in our ability to predict future changes in global fluxes and their impact on stratospheric ozone and climate. Pyle et al. (2011) reported measurements of bromocarbons from two land-based sites in Borneo covering 3 weeks in June and July 2008. The coastal measurements were characterised by large variability, from a background of 2 to 5 pmol mol^{-1} of $CHBr_3$ to occasional measurements of hundreds of pmol mol^{-1}. Measurements around the island were generally much lower and less variable, more consistent with the background of about 1 pmol mol^{-1}. The data were used to make an estimate of the regional emission strength of $CHBr_3$ which, depending on assumptions, ranged between 21 and 50 Gg/yr in SE Asia (10°N x 20°S, 90°E to 160°E). For the purpose of comparison we will also consider tetrachloroethylene (C_2Cl_4), which has predominantly industrial uses as a metal degreasing solvent, and dry cleaning and can be considered as a tracer of anthropogenic activity (Pyle et al., 2011).

How representative these Borneo measurements are of the whole SE Asia region is an important question and one that was addressed by the *Prime Expedition Scientific Cruise* in 2009 (PESC-09). Selected halocarbons, including the five bromomethanes detailed above, were measured in air samples collected in three different areas: the Strait of Malacca (SM),

the South China Sea (SCS) and the Sulu-Sulawesi Seas (SSS). Samples were collected at both coastal and open ocean locations, sometimes close to the sites mentioned in Pyle et al. (2011). The cruise and measurement details are presented in section 2. Results are presented and discussed in section 3.

2 Measurements

2.1 Cruise details

The PESC-09 cruise was conducted by the Malaysian Royal Navy and Malaysian Ministry of Science and Technology Innovation (MOSTI) and involved local government, private research agencies and public universities in Malaysia. The vessel used was the Kapal Diraja (Royal Ship) Perantau, which is designed and equipped for hydrographic surveying and for conducting meteorological and oceanographic observations. The cruise started from Port Klang (2°57' N101°20' E) in the Strait of Malacca, on 18th June and ended at, Kota Kinabalu (6°11'N116°10$^{'}$E) on 31st July. These paths were separated into four different legs: leg one (Port Klang-Labuan); leg two (Labuan-Layang-layang Island-Kota Kinabalu); leg three (Kota Kinabalu-Tawau) and leg four (Tawau- Kota Kinabalu). Figure 1 shows the ship's route together with the location of the 27 air sampling stations.

During the seven week cruise, several different oceanic regions were covered, including SM, SCS and SSS seas, and coastal regions of western and northern Borneo. Mangrove forest, sea grass beds and coral reefs dominate much of the coastline and, in northern Borneo in particular, there are areas of cultivated macroalgal beds along the coastline at sites such as Semporna, Kunak and Lahad Datu. The sampling locations were chosen to represent a variety of coastal and open ocean sites.

2.2 Sampling and measurements

Air was sampled through a 1/4″OD PFA tube located on the upper deck with the inlet ~10m above the ocean surface and adjusted at each sampling time to face the prevailing wind. Air was pumped into a pre-evacuated 3-litre canister (Restek SilcoCan™) using a compact, battery-operated diaphragm pump (Rasmussen) until the canisters were approximately two atmospheres above ambient pressure (approximately five minutes of sampling). Canisters were filled and vented at least three times, before a final fill which was kept for analysis. A total of 27 air samples were collected during the cruise, and these were shipped to the University of East Anglia (UK), for halocarbon analysis by GC-MS (gas chromatography - mass spectroscopy).

The samples were processed within four months of collection using a commercial thermal desorption system (Markes UNITY^{TM}/Air Server). The analytical technique was similar to that described by Worton et al. (2008). Air samples (1000 ml) were dried with a Nafion™ counter-flow dryer prior to collection and pre-concentration on a 2-bed adsorbent trap at -15^{o}C. The desorbed analytes were separated on a capillary column (Restek 100 m x 0.32 mm RTX 102) using a temperature programme of 30°C (2 min), 8°C/min to 150 $^{\circ}$C (16 min), 20°C/min to 220°C (5min). The mass spectrometer was operated in negative ion, chemical ionisation (NICI) mode using methane (≥99.99%) as the reagent gas. The quadrupole detector was run in single ion mode, monitoring *m*/*z* 35/37 for chlorinated, *m*/*z* 79/81 for brominated and *m*/*z* 127 for iodinated compounds. Samples were normally analysed twice and referenced to a working standard. The working standard was an aluminium cylinder containing dried ambient air at high pressure. The mole fractions of halocarbons in the working standard were determined by repeat comparison to calibrated gas standards supplied by NOAA-ESRL in electropolished stainless steel canisters (Essex Industries).

These comparisons are performed periodically and allow an assessment of any potential changes in the absolute mole fractions of halocarbons in our working standard over time. From comparisons with three separate NOAA standards: SX-3546 (comparison performed in 2008); SX-3570 (2010); and SX-3568 (2012) we believe the concentration of $CHBr_3$ in the working standard has declined by approximately 40% over the period October 2008-September 2012, whilst that of CH_2Br_2 has remained essentially unchanged (1.23 ± 0.07 pmol mol^{-1}, or 5.6%, 1σ). NOAA calibration data for the three mixed bromochloromethanes were only available for the 2010 and 2012 comparisons, but our analysis shows that the concentrations of CH_2ClBr and $CHClBr_2$ in the working standard have remained approximately constant (0.28 ± 0.004 pmol mol^{-1}, or 1.5%; and 1.18 ± 0.04 pmol mol^{-1}, 3.2% respectively) whilst that of $CHCl_2Br$ may have increased by around 15% (1.56 ± 0.17 pmol mol^{-1}, or 10.6%). The calibration factors applied to the PESC-09 data have been time-corrected as appropriate. This drift analysis makes the underlying assumption that the five bromocarbons are reliably stored in the Essex stainless steel cylinders.

The mole fractions reported here are on the latest NOAA scales for CH_2Br_2 (2004) and $CHBr_3$ (2003), and on a preliminary NOAA scale for CH_2BrCl, $CHBrCl_2$ and $CHBr_2Cl$ (Brad Hall, personal communication). The uncertainty in the absolute mole fractions in the working standard, based on combined uncertainties associated with the standard comparisons and NOAA's stated uncertainties was ± 6.5% for CH_2Br_2, ± 7.1% for $CHBr_3$, ± 7.5% for CH_2ClBr, ± 5.9% for $CHCl_2Br$ and ± 6.8% for $CHClBr_2$. Mean analytical precision of the actual PESC-09 samples was <3% for CH_2Br_2 and $CHBr_3$, <5% for $CHBrCl_2$ and $CHBr_2Cl$, and ~15% for CH_2BrCl, due to its low abundance and low response in NICI).

Chl-*a* in the surface seawater was measured using the Kapal Diraja (KD) Perantau's in-situ fluorometer attached to Sea-Bird SBE-911plus CTD (conductivity, temperature,

depth) system at all 27 sampling locations. The CTD equipment was operated together with a package consisting of a 24-place, 10-liter rosette frame, a 24-place water sampler (SBE32) and 24, 10-liter Niskin bottles sampler. This package was deployed at all stations. Several fluorometers, turbidity sensors and pH measurements were attached to the CTD. The CTD instrument was run and calibrated automatically at each station before sampling. The chl-*a* concentration was measured from 1 m to 20 m depth with 5 m intervals. Readings were taken at the sea surface approximately 1 m depth and have been compared with satellite-derived chl-*a* data from SeaWIFS (Sea-Viewing Wide Field-of-view Sensor) and MODIS (Moderate Resolution Imaging Spectroradiometer). Chl-*a* derived from ocean colour measurements made during overpasses of the SeaWIFS and Aqua-MODIS satellite sensors were used to determine apparent chl-*a* values in the nearest 9x9 km grid square to each sampling point. The corresponding monthly average chl-*a* values (i.e. those for either June or July) were used, obtained from the NASA Goddard 'Giovanni' on-line database (http://oceancolor.gsfc.nasa.gov/SeaWiFS/). Shorter averaging periods are available (e.g. 8-day) but were found to be insufficient for full coverage of the cruise track given the width of the viewing swath, the level of missing data on several overpasses, and differences between satellite sensors in ocean colour-derived chl-*a*. There is a substantial difference in both the temporal and spatial scales between the monthly-averaged and 9x9 km grid-box averaged satellite measurements and the near-instantaneous *in situ* 'spot' measurements. As an indication of the level of uncertainty (at least that related to spatial scales) the standard deviation of satellite-determined chl-*a* was calculated for the eight to ten grid boxes surrounding and including the target grid box, depending on the values at each location (negative values were not considered).

3. Results and Discussion

In the following sections we will, first, present an overview of the halocarbon data collected during PESC-09 (section 3.1). We then discuss possible causes of any observed variability, focussing on an analysis of air parcel trajectories and *in situ* measurements of chl-*a*, which are a possible proxy for biological activity (section 3.2). In section 3.3 we explore correlations between the measured species and provide a rough estimate of regional bromoform emissions. Finally (section 3.4) we use the data to investigate the potential contribution of VSLS to stratospheric bromine loading.

3.1 Halocarbon measurements

Mean and standard deviation of the measured halocarbon concentration at each site are given in Table 1 along with some comparison with data from the literature. Figure 2 shows the concentrations of brominated compounds ($CHBr_3$, CH_2Br_2, $CHBr_2Cl$, $CHBrCl_2$ and CH_2BrCl) at each of the cruise sampling sites, whose locations are marked on Figure 1. The most abundant bromine compound was $CHBr_3$, with mean concentrations from around 1pmol mol^{-1} to more than 5 pmol mol^{-1} (mean = 1.85 pmol mol^{-1}, max = 5.2 pmol mol^{-1}). Most measurements are between 1 and 2 pmol mol^{-1}. The mean mixing ratio of $CH_2Br_2$was 1.23 pmol mol^{-1} (max = 2.21), with the minor species $CHBr_2Cl$, $CHBrCl_2$ and CH_2BrCl having mixing ratios in the mean 0.1 to 0.9 pmol mol^{-1}. For the anthropogenic tracer C_2Cl_4, mixing ratios varied only between 0.9 and 1.0 pmol mol^{-1}. The PESC-09 measurements are generally within the range of previous measurements in tropical regions.

241 **3.2 Regional analysis**

242 **3.2.1 Strait of Malacca** (Stations 1-4).

243 PESC-09 took place during the South West Monsoon (SWM) when sea surface temperatures
244 are slightly warmer (28-32^{o}C, May/June) than in the North West Monsoon (NWM) (25-29°C,
245 December/January). Tan et al. (2006) report that chl-*a* in the Strait of Malacca shows
246 seasonal variability with concentrations increased by as much as a factor of two (0.57 mgm^{-3}
247 in August and 1.38 mgm^{-3} in January 1992-2002 monthly average) during NEM compared to
248 SWM.

249 The highest concentrations of $CHBr_3$ were observed at the beginning of the cruise in the
250 Strait of Malacca (SM). The mean concentration in samples 2-4 was 4.4 pmol mol^{-1}, which is
251 similar to the levels in the same region reported by Yokouchi (1997). The enhanced levels
252 may be related to the high population of macro and micro algae such as phytoplankton and
253 seaweeds at coastal areas, especially in the region of 1-2^{o}N, 102-103^{o}W. Previous studies on
254 chl-*a* in the SM were influenced by nutrient input from rivers of Sumatra (Tan et al., 2006).
255 CH_2Br_2, $CHCl_2Br$, $CHClBr_2$ and $CHCl_3$ were also enhanced in samples 2-4, which is
256 indicative of similar sources.

257

258 **3.2.2 South China Sea (Stations 5 to 14)**

259 Measurements in the SCS show fairly uniform and relatively low mixing ratios for all
260 brominated compounds. For example, the mean values for $CHBr_3$, CH_2Br_2 and $CHBr_2Cl$ were
261 1.46, 1.12 and 0.35 pmol mol^{-1} respectively, with no significantly enhanced values. The
262 prevailing wind direction for most samples collected along this section of the cruise was
263 westerly, so the influence of any local coastal emissions would likely be low.

3.2.3 Sulawesi and Sulu Seas (Stations 15-27)

Slightly higher concentrations of bromocarbons were observed during the cruise through the SSS, especially at Station 22 and 24 where $CHBr_3$ concentrations were 2.37 and 2.60 pmol mol^{-1} respectively. During this period the ship passed near to coastal sites at Semporna (station 22), Kunak (19, 20, 21, 27) and Tawau (24, 26). The coastal areas near Semporna and Kunak have significant seaweed biomass, with cultivated *Kappaphycus* and *Eucheuma* at Semporna and *Sargassum* and other brown algae at Kunak. Samples 17 and 21 had slightly elevated levels of C_2Cl_4, suggesting a possible influence from local anthropogenic sources.

Pyle et al. (2011) measured $CHBr_3$ concentrations at Kunak ranging from a typical background of 2-5 pmol mol-1, but high concentration up to 60 pmol mol^{-1} (the latter were attributed to measurement very close to local emissions). During their short measurement period in July 2008 the air flow was predominantly from the south east, with back-trajectories showing air travelling from northern Australia, over the Timor and East Java Seas and up the eastern coast of Borneo. The authors speculated that these are areas of high biological activity, with both the warm ocean and extensive coastline providing significant sources of halocarbons. Despite similar air mass back-trajectories and sampling in similar locations, we did not measure the very high levels of $CHBr_3$ reported by Pyle et al. (2011). For example, at station 27, back-trajectories did not indicate that air flow had passed any seaweed or high nutrient area.

3.3 Drivers of variability

The data collected during PESC-09 show relatively small variability, consistent with the ship data reported by Yokouchi et al. (1997) over the western Pacific and South East Asia (see Table 1). For example, Yokouchi observed mixing ratios of $CHBr_3$ of 0.32 to 7.1 pmol mol^{-1} which is similar to our study, with a range of 1.85-5.25 pmol mol^{-1} for $CHBr_3$. This contrasts with the study of Yokouchi et al. (2005) over western Pacific and Java Island, who observed high mixing ratios with a range of 16.3 to 31.4 pmol mol^{-1} at Christmas Island, and 4.2 to 43.6 pmol mol^{-1} at San Cristobal Island. Pyle et al. (2011) also observed high mixing ratios of $CHBr_3$ in Malaysian Borneo (near to station 21 and 27 in this study), with a range of 2 to 60 pmol mol^{-1}. It seems likely that these latter studies both included data collected close to emission sources.

Atmospheric variability is driven by various factors including wind direction, atmospheric lifetime, proximity to local sources and temporal variation of flux rates. Changes in VSLS emissions could arise from a number of complex factors. Emissions of VSLS are predominantly biogenic, with the ocean being the most important source (Baker et al., 2000; Quack et al., 2004). Proximity to local seaweed beds (including seaweed farms) is likely to be an important influence in coastal regions. In the case of microalgae, their abundance and distribution in seawater are affected by nutrient supplies and sea surface temperatures, while sea-air fluxes of VSLS are determined by meteorological parameters including wind speed. Chl-*a* can be used as a simple proxy for biological activity, possibly producing halocarbons, which may be emitted into the atmosphere, depending on concentrations and wind speed.

3.3.1 Meteorological variability

A major factor controlling the variability of the halocarbon concentrations during the cruise is the wind direction. Figure 3 shows selected 10-day air mass back trajectories for seven of the cruise sampling locations calculated from the NOAA HYSPLIT model (R. R. Draxler and G. D. Rolph, HYSPLIT- Hybrid Single-Particle Lagrangian Integrated Trajectory), available at http://www.arl.noaa.gov/ready.html). In all cases the large-scale structure is consistent. Air masses arriving at the sampling locations originated to the south east and have likely been influenced by emissions from shallow, warm seas, including the South Java Sea. There is therefore likely to be little variability associated with transport from different large-scale emission regions, although local emissions close to the sampling locations could still be important in driving local variability. For example, the trajectories arriving at site 22, near Sipadan Island, or at station 19, near Kunak, are very likely to have been influenced by the seaweed beds in that area. A similar conclusion was reached by Pyle et al. (2011) based on their coastal Kunak measurements in June 2008, made one year earlier than the PESC-09 cruise and the origins of the measured air masses were very similar in both years.

3.3.2 Biological activity

Chl-*a* was also measured at 60 sites including 27 sites where halocarbons are measured during the cruise, both *in situ* from the ship and remotely from satellite sensors. We compare the chl-*a* measurements with the halocarbon data to explore possible biological drivers of variability. Figure 1 plots the monthly average chl-*a* across the region from SeaWiFS for June 2009 overlaid with the sampling stations. High chl-*a* levels are commonly observed along the coastlines, seemingly indicating high phytoplankton abundance. Indeed high satellite-derived chl-*a* values were evident in the Strait of Malacca, where the highest $CHBr_3$

was measured. However, a plot of ocean colour-derived chl-*a* from the two satellite sensors versus *in situ* chl-*a* (Figure 4) shows significant disagreement between the remotely-sensed and *in situ* measurements. The standard deviations from the target grid box and those surrounding it are in the range of 1.1 to 32.4 mgm^{-3} for MODIS and 0.1 to 18.2 mgm^{-3} for SeaWiFS.

In Figure 4, the filled symbols denote samples in which the turbidity was >0.5 FTU (Formazin turbidity unit), whereas open symbols denote low turbidity (<0.5 FTU). It is apparent that the low turbidity samples display a relatively compact relationship between remotely-sensed and *in situ* chl-*a* and with absolute values that are in good quantitative agreement. Indeed a linear regression on the lower turbidity samples yields a gradient of 1.0 (standard error of 0.1) and an r^2 value of 0.88. The points that do not follow the positive linear regression line are characterised by satellite chl-a concentrations greater than 1 mg m^{-3}, and turbidities greater than 0.5 FTU, implying that the satellite sensors over-estimate chl-*a* under such conditions. Indeed the *in situ* measurements showed that ship-board measurements of chl-*a* are lower than those made in the open ocean. We reiterate (refer back to Section 2.2) that there are difficulties in comparing coarse satellite data with *in situ* measurements, but believe this type of comparison still provides valuable information from a data-sparse region.

Plots of bromocarbon air concentration versus satellite chl-*a* concentration (Figure 5) show a positive correlation, with the highest mixing ratios of $CHBr_3$ and CH_2Br_2 associated with above average chl-*a* values (> 5 mgm^{-3}) for MODIS and SeaWiFS satellites. Both satellite chl-*a* products show R values > 0.6 against $CHBr_3$ and CH_2Br_2 (also $CHBr_2Cl$ for MODIS) but other species show little correlation for both satellite chl-*a* products. *In situ* chl-*a* concentrations show negative correlation for all bromocarbons species with r=-0.26

359 ($p>0.01$) and $r=-0.21$ ($p>0.01$) for $CHBr_3$ and CH_2Br_2, respectively (see figure 5). The exact
360 reason for the weak correlation of the bromocarbons and the *in situ* chl-*a* data is unclear.

361 The above finding is not necessarily surprising even if phytoplankton are a source of
362 such gases, since a connection between bromocarbons measured in the marine atmospheric
363 boundary layer and sub-surface biology may be dependent on other factors including wind
364 speed. Furthermore, the observed halocarbon concentrations might originate over a wide
365 geographic area and are not necessarily driven solely by localised emissions. In this context,
366 satellite-derived chl-*a*, also providing information from a wider area, may potentially be more
367 relevant than *in situ* measurements. Although turbidity measurements in the Strait of Malacca
368 (average of 3.3 FTU) were significantly higher than those in the South China Sea (average of
369 0.3 FTU; Table 1), coinciding with high $CHBr_3$, the turbidity was almost as high close to land
370 near Semporna (average of 2.1 FTU for Stations 24-27), but with little evidence of
371 substantially enhanced halocarbons in the latter region due to the lower marine productivity
372 especially at the coastal and open ocean region of SCS (Figure 1). We conclude that
373 halocarbon concentrations are generally somewhat higher close to land and also higher in the
374 Strait of Malacca, thus a connection to the coastal zone is suspected, but there is little
375 evidence to connect this directly to open ocean microorganisms.

376

377 **3.4 Emission ratios**

378 Significant correlations between brominated halocarbons have been observed in coastal air
379 measurements suggesting that these gases have come from the same sources (Yokouchi et al.,
380 2005; O'Brien et al., 2009; Carpenter et al., 2009). Several studies have exploited these
381 correlations to explore the possible source strengths of the individual species. Carpenter et al.

(2003), Yokouchi et al. (2005) and O'Brien et al. (2009) all show that a log-log plot of $CH_2Br_2/CHBr_3$ versus $CHBr_3$ often shows a straight line with the ratio $CH_2Br_2/CHBr_3$ increasing with decreasing $CHBr_3$. Atmospheric ratios of $CH_2Br_2/CHBr_3$ are often interpreted in the light of their differing atmospheric lifetimes, which are about 26 days for $CHBr_3$ and 120 days for CH_2Br_2 (Montzka et al., 2011). The relationship between $CHBr_3$ and other somewhat longer-lived brominated halocarbons such as $CHBr_2Cl$ also showed similar patterns, for example $CHBr_2Cl/CHBr_3$ would be higher at lower concentration of $CHBr_3$. Since $CHBr_3$ has the shorter lifetime of the two species, an increase in the ratio would be consistent with more aged air masses, in which $CHBr_3$ has been removed at a faster rate. Yokouchi et al. (2005) used the minimum ratio of $CH_2Br_2/CHBr_3$ to define the ratio of the emission sources by assuming that the emissions came from the common sources and are constant on a regional scale. If the global emission of CH_2Br_2 is known, then that of $CHBr_3$ can be inferred. However the emission ratio for $CH_2Br_2/CHBr_3$ in the open ocean is different (i.e. higher) to that in coastal areas and so the assumption of a single characteristic seawater ratio is invalid, along with the extrapolation of source strength.

Figure 6 shows the relationships between CH_2Br_2 and $CHBr_3$ and between $CHBr_2Cl$ and $CHBr_3$ for each data set. Correlations are strong between CH_2Br_2 and $CHBr_3$ (correlation coefficient, $r = 0.9$), $CHBr_3$ and $CHBr_2Cl$ ($r = 0.7$) and $CHBr_3$ and $CHBrCl_2$ (correlation coefficient $r = 0.5$) (not shown in the figure). These variations in correlation are consistent with the relationships observed in recent studies of the strength of emission of these different compounds from a range of Malaysian seaweeds (Leedham et al., 2013; Seh-Lin Keng et al., 2013). Figures 7a and 7b show the concentration ratios of $CH_2Br_2/CHBr_3$ and $CHBr_2Cl/CHBr_3$ plotted against $CHBr_3$ on a log-log scale, with both ratios increasing linearly

405 as $CHBr_3$ decreases; $CHBr_3$, with its shorter lifetime, is a possible measure of time since co-
406 emission. These figures are consistent with those reported by Yokouchi et al. (2005).

407 Yokouchi et al. (2005), following McKeen and Liu (1993), used plots of pairs of
408 ratios, e.g. $CHBr_3/CH_2Br_2$ versus $CHBr_2Cl/CH_2Br_2$, where CH_2Br_2 has the longest lifetime, to
409 explore the possible emission strengths of the individual species. Making a number of
410 assumptions, in such a plot the location of individual points in ratio space is determined by
411 the emission ratio at an (assumed) common regional source and by the ratio of the rates of
412 chemical removal and mixing into the 'background' atmosphere. Assuming that the emission
413 source strength of one species is known, that of the others can be obtained using the ratio
414 determined from the plot. Using this method, O'Brien et al. (2009) estimated a global
415 emission of bromoform of 823-1404 Gg/yr (values depend *inter alia* on the assumed CH_2Br_2
416 emissions) using data collected at Cape Verde in June 2006. This emission is much higher
417 than estimates in Ko et al. (2003), or in Warwick et al. (2006). However, Pyle et al. (2011)
418 suggest that it is not reasonable to derive global emission estimates from regional data for a
419 short-lived species such as bromoform. They showed that data from Borneo could instead
420 only be used to constrain regional emissions.

421 Using data from the cruise, $CHBr_3/CH_2Br_2$ is plotted against $CHBr_2Cl/CH_2Br_2$ in
422 Figure 7b. The left side of the triangle is the 'dilution line' (the 1:1 slope for mixing into a
423 zero background) and the 'chemical decay line', defined by the ratio of lifetimes of individual
424 species due to photochemistry, is the right hand line. The intersection of these 2 lines, a point
425 typically chosen to allow the lines to encompass the majority of the data, defines the emission
426 ratios. Nearly all the data falls into a triangle whose vertex for $CHBr_3/CH_2Br_2$ takes a value
427 of 5 (point D on the figure). This is about half the value reported by Yokouchi et al. (2005)
428 and O'Brien et al. (2009) but similar to the result obtained by Brinckmann et al. (2012) based

on data collected in a recent western Pacific cruise. If we assume that this emission ratio of 5 is appropriate to the SE Asian Region, (10°N to 20°S, 90°E to 160°E, as used by Pyle et al. (2011)) and recalling that the air mass histories in the two periods of these two studies are quite similar, then we could derive an emission estimate for $CHBr_3$ from the regional CH_2Br_2 emission. That value is not observationally constrained; instead we use the SEA regional CH_2Br_2 emission from an updated version of the Warwick et al. (2006) inventory (as used by Yang et al., 2014). As before, spatially uniform ocean emissions of CH_2Br_2 are assumed in the tropics, but emissions are halved so that the global total of 57 Gg CH_2Br_2/yr is more consistent with the recent studies of Liang et al. (2010) and Ordonez et al. (2012). In that case, with a SEA CH_2Br_2 emission of 6.4 Gg/yr, we obtain a regional emission, based on point D from figure 7b, of about 32 Gg/yr of $CHBr_3$. This value is within the range obtained by Pyle et al (2011), who estimated emissions of $CHBr_3$, for the same area, to be between 21 and 50 Gg/yr. It is also consistent with the recent work of Ashfold et al. (2014), who estimated a total tropical $CHBr_3$ emission of 225 Gg/yr; simply scaling this tropical number down (using the ratio of areas) to the SEA region considered here implies a $CHBr_3$ emission of 33 Gg/yr. Our estimates, and those of Pyle et al. (2011) and Ashfold et al. (2014), are all much less than the regional value in Warwick et al. (2006). To be more confident about our emission value would require, amongst other things, improved estimates of the CH_2Br_2 emission. However, the consistency of the calculations does suggest that useful constraints on regional estimates can be obtained based on McKeen and Liu (1993) plots.

3.5 Total bromine

The cruise data can be used to give an upper limit on the amount of bromine which could potentially reach the stratosphere, i.e. by summing the measured bromine mixing ratios and

453 weighting by the number of bromine atoms. The mean VSLS-derived bromine ($[Br]_{VSLS}$) in
454 the 27 samples was 8.9 ± 3.7 pmol mol^{-1}. There is some regional variability as discussed
455 earlier, with SM having the highest $[Br]_{VSLS}$ (mean = 17.8 pmol mol^{-1}) compared to other
456 sampled areas. Of this 8.9 pmol mol^{-1}, $CHBr_3$ contributes ~65% and CH_2Br_2 25%. This is
457 similar to results compiled by Montzka et al. (2011) for which an average total bromine from
458 the same gases in the tropical marine boundary layer (mostly from open ocean
459 measurements) is given as 8.4 pmol mol^{-1} with a range of 3.6–13.3 pmol mol^{-1}. With the
460 exception of the Strait of Malacca, there does not appear to be a large regional enhancement
461 of $[Br]_{VSLS}$ in our data, despite the cruise having taken place mostly within 50 km of the
462 coast. The data do not suggest that this part of SE Asia is a 'hot spot' for emissions.

463 The $[Br]_{VSLS}$ measured during the PESC-09 cruise are likely to account for some of
464 the 'missing' bromine entering the stratosphere, assuming conservative transport of the
465 constituent bromine either in the form of the source gas itself, or as brominated product
466 gases.

467

468 **4. Conclusions**

469 We report *in situ* halocarbon and ancillary data obtained during a research cruise of
470 the Perantau in June and July 2009. The cruise covered the Strait of Malacca, the South China
471 Sea and the Sulu and Sulawesi Seas. These are warm, shallow ocean areas and contain
472 conditions likely to support high halocarbon production and emission to the atmosphere. The
473 region is also important as a location of the strongest convection, therefore it thus represents
474 potentially an important source region for the transport of marine boundary layer
475 concentrations of VSLS to the upper troposphere and stratosphere.

476 Data were collected at 27 sites during the cruise. High bromoform concentrations (4-5
477 pmol mol^{-1}) were measured in the nutrient rich Strait of Malacca. Otherwise concentrations
478 were generally between 1 and 2 pmol mol^{-1}. This is consistent with an earlier cruise reported
479 by Yokouchi et al. (1997). Slightly higher concentrations were measured close to seaweed
480 farms in Semporna but nowhere on the cruise did we find very high concentrations similar to
481 those reported by Pyle et al. (2011) at a coastal site at Kunak, believed to be close to emission
482 sources. Further, there is no evidence from the cruise data that local emission sources in this
483 region lead to widespread, elevated concentrations ('hotspots') which might make a
484 contribution to stratospheric input out of proportion to the area of the region.

485 Our measurements of other compounds, including the less often reported mixed
486 chloro-bromocarbons, are also reasonably consistent with the few other studies in the region
487 (e.g. Quack and Suess, 1999; Yokouchi et al., 1997, see table 1). Our typical concentrations
488 of CH_2Br_2 ~1 pmol mol^{-1}, $CHBr_2Cl$ ~0.2-0.4 pmol mol^{-1}, $CHBrCl_2$ ~0.2-0.3 pmol mol^{-1} and
489 CH_2BrCl ~0.1-0.2 pmol mol^{-1} lead to a $[Br]_{VSLS}$ of 8.9 pmol mol^{-1}. This is close to values
490 obtained by Sala et al., (2014) from measurements collected in the planetary boundary layer
491 of the same region during the SHIVA campaign (7.8 and 9.1 pmol mol^{-1} using two separate
492 instruments). The similarity suggests boundary layer VSLS mixing ratios in this important
493 region are beginning to be better characterised.

494 The bromocarbons were well correlated, suggesting common sources. Previously,
495 such relationships have been used to obtain global emission estimates. For a short-lived gas
496 like bromoform, with an atmospheric lifetime of ~26 days, we do not think this approach is
497 suitable; the footprint sampled by the cruise is regional at most. Instead, we used an approach
498 as applied by Yokouchi et al. (2005) to provide a very rough estimate of the regional (S.E.
499 Asia) emission ratio of bromoform to dibromomethane of about 5. Using the

dibromomethane emissions from Liang et al. (2010) leads to bromoform emissions of 32 Gg yr^{-1} for S.E. Asia (10°N to 20°S, 90°E to 160°E), which is in reasonable agreement with the recent estimates from Pyle et al. (2011) and Ashfold et al. (2014). Much more data, not least on CH_2Br_2 emissions, would be required to confirm this estimate, but the use of species correlations for regional emission estimates looks to be a promising approach.

Chl-*a* was also measured on the cruise. There was little obvious correlation between this and the measured atmospheric halocarbon concentrations. Satellite measurements of chl-*a* suggested high values in the Strait of Malacca, coinciding with high turbidity and high halocarbon concentrations. However, it seems likely that the satellite data were affected by the high turbidity in these waters, and the underwater *in situ* chl-*a* measurements were similar to those observed in the open sea. It seems likely that the higher halocarbon concentrations in the Strait maybe result from local influence of the nearby coastal areas and land masses.

The seas around South East Asia are important for a number of atmospheric processes, including both convection and the emission of brominated halocarbons. Measurements of brominated halocarbons in this region are sparse, and despite the new measurements reported here, the region remains data poor.

Acknowledgements

We would like to thank MOSTI (Malaysian Government) for giving opportunities and financial support for University of Malaya (UM) to participate in this scientific cruise and other Malaysian public universities who helping during sampling. The Malaysian Royal Navy is thanked for their help and assistance in all aspects of the cruise. We also thank the European FP7 project SHIVA (grant 226224), NERC, NERC-NCAS and the British Council, through a PMI2 grant, for their support. Neil Harris would like to thank NERC for his Research Fellowship; Emma Leedham and Matt Ashfold thank NERC for studentships and Ministry of Higher Education Malaysia (KPT's) ERGS grant ER025-2013A. Finally, we also would like to thank Universiti Kebangsaan Malaysia (UKM) ICONIC-2013-004 grant, MOSTI's e-science grant 04-01-02-SF-0752 for University Kebangsaan Malaysia (UKM) and UKM GGPM-2013-080 who participated in this cruise.

References

Ashfold, M. J, Harris, N. R. P., Robinson, A. D., Warwick, N. J., and Pyle, J. A., Estimates of tropical bromoform emissions using an inversion method. Atmos. Chem. Phys., 14, 979-994, 2014.

Baker, A. R., S. M. Turner,W. J. Broadgate, A. Thompson, G. B. McFiggans, O. Vesperini, P. D. Nightingale, P. S. Liss, and T. D. Jickells , Distribution and sea-air fluxes of biogenic trace gases in the eastern Atlantic Ocean, Global Biogeochem. Cycles, 14(3), 871–886, 2000.

Brinckmann, S., Engel, A., Bönisch, H., Quack, B., Atlas, E., Short-lived brominated hydrocarbons – observations in the source regions and the tropical tropopause layer, Atmos. Chem. Phys., 12, 1213-1228, 2012

Butler, H. J., King, B. D., Lobert, M. J., Montzka, A. S., Yvon-Lewis, A. S., Hall, D. B., Warwick, Mondeel, J. D., Aydin, M., Elkins, W. J., Oceanic distribution and emissions of short-lived halocarbons, Global Biogeochem. Cycles, 21, 1023, doi:10.1029/2006GB002732, 2007a.

Carpenter, L. J., Liss, P. S., and Penkett, S. A.: Marine organohalogens in the atmosphere over the Atlantic and Southern Oceans, J. Geophys. Res., 108(D9), 4256, doi:10.1029/2002JD002769, 2003.

566 Carpenter, L. J., Jones, C. E., Dunk, R. M., Hornsby, K. E., and Woeltjen, J.: Air-sea fluxes
567 of biogenic bromine from the tropical and North Atlantic Ocean, Atmos. Chem. Phys., 9,
568 1805–1816, 2009.
569
570 Dorf, M., J. H. Butler, A. Butz, C. Camy-Peyret, M. P. Chipperfield, L. Kritten, S. A.
571 Montzka, B. Simmes, F. Weidner, and K. Pfeilsticker, Observations of long-term trend in
572 stratospheric bromine reveal slowdown in growth, Geophys. Res, Lett., 33, L24803,
573 doi:10.1029/2006GL027714, 2006.
574
575 Fueglistaler, S., Wernli, H. and Peter, T., Tropical troposphere to stratosphere transport
576 Kinferred from trajectory calculations, J. Geophys. Res., 109, D03108,
577 doi:10.1029/2003JD004069, 2004.
578
579 Fueglistaler, S., Dessler, A. E., Dunkerton, T. J., Folkins, I., Fu, Q., and Mote, P. W.:
580 Tropical Tropopause Layer, Rev. Geophys., 47, RG1004, 443, 2009.
581
582 Gettelman, A., Salby, M.L. and Sassi, F., The distribution and influence of convection on the
583 tropical tropopause region, J. Geophys. Res., 107, 4080, doi:10.1029/2001JD001048, 2002.
584
585 Ko, M. K. W., Poulet, G., Blake, D. R., Boucher, O., Burkholder, J. H., Chin, M., Cox, R. A.,
586 George, C., Graf, H.-F., Holton, J. R., Jacob, D. J., Law, K. S., Lawrence, M. G., Midgley, P.
587 M.,Seakins, P. W., Shallcross, D. E., Strahan, S. E., Wuebbles, D. J., Yokouchi, Y., and
588 contributors: Very Short-Lived Halogen and Sulfur Substances, Scientific Assessment of

589 Ozone Depletion: 2002, World Meteorological Organization Global Ozone Research and
590 Monitoring Project – Report No. 47, Geneva, Switzerland, 2.1–2.57, 2003.

591

592 Laturnus, F and Adams, F. C.,: Methyl halides from Antarctic macroalgae. Geophys. Res.
593 Lett, 25, 773-776, 1998.

594

595 Leedham, E. C., Hughes, C., Keng, F. S. L., Phang, S.-M., Malin, G., and Sturges, W. T.:
596 Emission of atmospherically significant halocarbons by naturally occurring and farmed
597 tropical macroalgae, Biogeosciences, 10, 3615–3633, doi:10.5194/bg-10-3615-2013, 2013.

598

599 Liang, Q., Stolarski, R. S., Kawa, S. R., Nielsen, J. E., Douglass, A. R., Rodriguez, J. M.,
600 Blake, D. R., Atlas, E. L., and Ott, L. E.: Finding the missing stratospheric Bry: a global
601 modeling study of CHBr3 and CH2Br2, Atmos. Chem. Phys., 10, 2269–2286,
602 doi:10.5194/acp-10-2269-2010, 2010.

603

604 McKeen, S. A. and Liu, S. C.: Hydrocarbon ratios and photochemical history of air masses,
605 Geophys. Res. Lett., 20, 2363–2366, 1993.

606

607 Montzka, S.A., S. Reimann, A. Engel, K. Krüger, S. O'Doherty, W.T. Sturges, Ozone-
608 Depleting Substances (ODSs) and Related Chemicals, Chapter 4 in *Scientific Assessment of*
609 *Ozone Depletion: 2010, Global Ozone Research and Monitoring Project–Report No. 52*, 516
610 pp., World Meteorological Organization, 2011.

611

612 Moore, R.M., Webb, M., Tokarczyk, R. And Wever, R. Bromoperoxidase and
613 iodoperoxidase enzumes and production of halogenated methanes in marine diatom cultures.
614 Journal of Geophysical Research C: Oceans vol. 101(C9) pp.20899-20908, 1996.

615

616 O'Brien, L. M., Harris, N. R. P., Robinson, A. D., Gostlow, B., Warwick, N., Yang, X., and
617 Pyle, J. A.,Bromocarbons in the tropical marine boundary layer at the Cape Verde
618 Observatory measurements and modelling, Atmos. Chem. Phys., 9, 9083–9099,
619 doi:10.5194/acp-9-9083-9099, 2009.

620

621 Ordóñez C., Lamarque, J.-F., Tilmes, S., Kinnison, D. E., Atlas, E. L., Blake, D. R., Sousa
622 Santos, G., Brasseur, G., and Saiz-Lopez, A.: Bromine and iodine chemistry in a global
623 chemistry-climate model: description and evaluation of very short-lived oceanic sources,
624 Atmos. Chem. Phys., 12, 1423–1447, doi:10.5194/acp-12-1423-2012, 2012.

625

626 Pyle, J. A., Ashfold, M. J, Harris, N. R. P., Robinson, A. D., Warwick, N. J., Carver, G. D.,
627 Gostlow, B., O'Brien, L. M., Manning, A. J., Phang, S. M., Yong, S. E., Leong, K. P., Ung,
628 H. E., and Ong, S., Bromoform in the tropical boundary layer of the Marintime Continent
629 during OP3. Atmos. Chem. Phys., 11: 529-542, 2011.

630

631 Quack, B. and Suess, E.: Volatile halogenated hydrocarbons over the western Pacific 43^{o} and
632 4^{o} N, J. Geophys. Res., 104, 1663– 1678, 1999.

633

634 Quack, B., Atlas, E., Petrick, G., Stroud, V., Schauffler, S., and Wallace, D. W. R.: Oceanic
635 bromoform sources for the tropical atmosphere, Geophys. Res. Lett., 31, L23S05,
636 doi:10.1029/2004GL020597, 2004.
637
638 Salawitch, R. J, Atmospheric chemistry: Biogenic bromine, Nature, 439, 275–277,
639 doi:10.1038/439275a, 2006.
640
641 Sala, S., Bönisch, H., Keber, T., Oram, D. E., Mills, G., and Engel, A.: Deriving an
642 atmospheric budget of total organic bromine using airborne in-situ measurements from the
643 Western Pacific during SHIVA, Atmos. Chem. Phys. Discuss., 14, 4957-5012,
644 doi:10.5194/acpd-14-4957-2014, 2014.
645
646 Seh-Lin Keng, F., Phang, S. M., Abd Rahman, N., Leedham, E., Hughes, C., Pyle, J. A.,
647 Harris, N. R. P., Robinson, A., and Sturges, W. T.: Volatile halocarbon emissions by three
648 tropical brown seaweeds under different irradiances, J. Appl. Phycol., 25, 1377–1386,
649 doi:10.1007/s10811-013-9990-x, 2013.
650
651 Sturges, W. T., Sullivan, C. W., Schnell, R. C., Heidt, L. E., and Pollack, W. H.:
652 Bromoalkane production by Antartic ice algae. Tellus B 45, 120-126. 1993.
653
654 Tan, C. K., Ishizaka, J., Matsumura, S., Yusoff, F. M., and Mohamed, M. I. H.: Seasonal
655 variability of SeaWiFS chlorophyll a in the Malacca Strait in relation to Asian monsoon.
656 Continental Shelf Res., 26: 168-178, 2006.

657 Warwick, N. J., Pyle, J. A., Carver, G. D., Yang, X., Savage, N. H., O'Connor, F. M., and
658 Cox, R. A.: Global modelling of biogenic bromocarbons, J. Geophys. Res., 111, D24305,
659 doi:10.1029/2006JD007264, 2006.

660

661 World Meteorological Organization (WMO)/United Nations Environment Programme
662 (UNEP): Scientific Assessment of Ozone Depletion: 2006, World Meteorological
663 Organization, Global Ozone Research and Monitoring Project, Report No. 50, Geneva,
664 Switzerland, 2007.

665

666 Worton, D. R., Mills, G. P., Oram, D. E., and Sturges, W. T.: Gas chromatography negative
667 ion chemical ionization mass spectrometry: application to the detection of alkyl nitrates and
668 halocarbons in the atmosphere, J. Chromatogr. A, 1201, 112–119, 2008.

669

670 Yang, Y., Abraham, N. L., Archibald, A. T., Braesicke, P., Keeble, J., Telford, P., Warwick,
671 N. J and Pyle, J. A: How sensitive is the recovery of stratospheric ozone to changes in
672 concentrations of very short lived bromocarbons? Atmos. Chem. Phys. Discuss., 14, 1919–
673 1969, submitted, 2014.

674

675 Yokouchi, Y., Mukai, H., Yamamoto, H., Otsuki, A., Saitoh, C., and Nojiri, Y., Distribution
676 of methyl iodide, ethyl iodide, bromoform, and dibromomethane over the ocean (east and
677 southeast Asian seas and western Pacific). J. Geophys Res, 102, 8805-8809, 1997.

678

679 Yokouchi, Y., Hasebe, F., Fujiwar, M., Takashima, H., Shiotani, M., Nishi, N., Kanaya Y.,
680 Hashimoto, S., Fraser, ,P., Toom-Sauntry, D. Mukai, H., and Nojiri, Y. Correlations and
681 emission ratios among bromoform, dibromochloromethane, and dibromomethane in the
682 atmosphere. J. Geophys Res, 110, D23309, doi:10.1029/2005JD006303, 2005.

683

684

685

686

687

688

689

690

691

692

693

694

695

696

697

698

699

700

701

702

703

704

705

706 **List of figures**

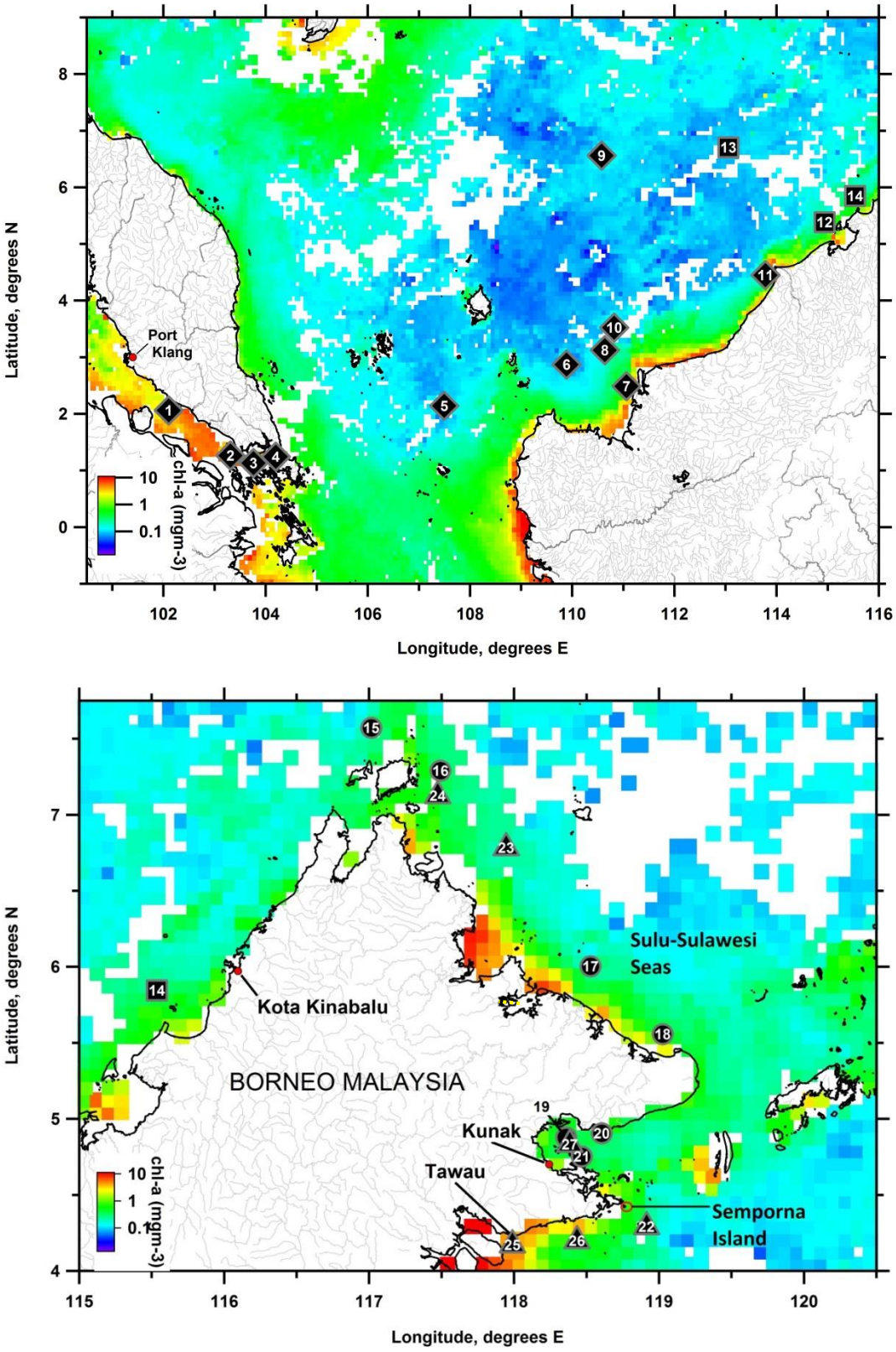

707

708

709 **Figure 1:** Sampling locations overlaid with SeaWiFS chl-a during PESC-09 (Labels:
710 diamond = 1st leg; square = 2nd leg; circle = 3rd leg and triangle = 4th leg).

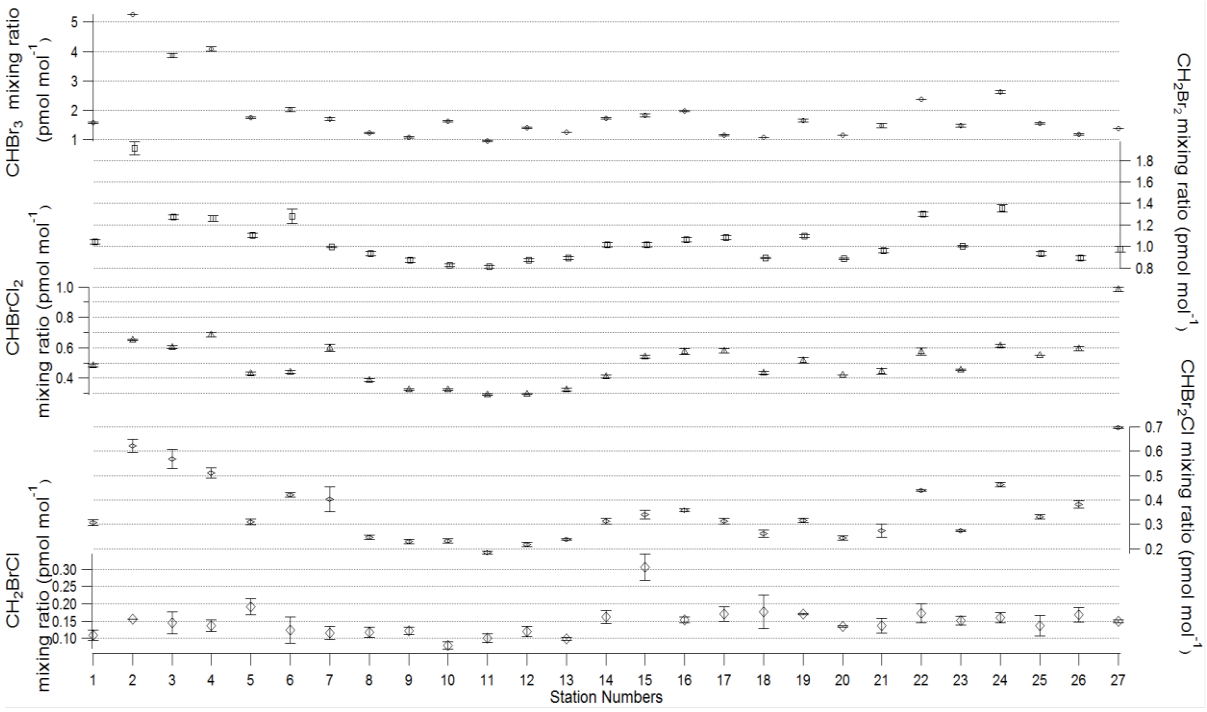

711

712 **Figure 2:** Bromocarbon mixing ratios for each station during PESC-09.

713

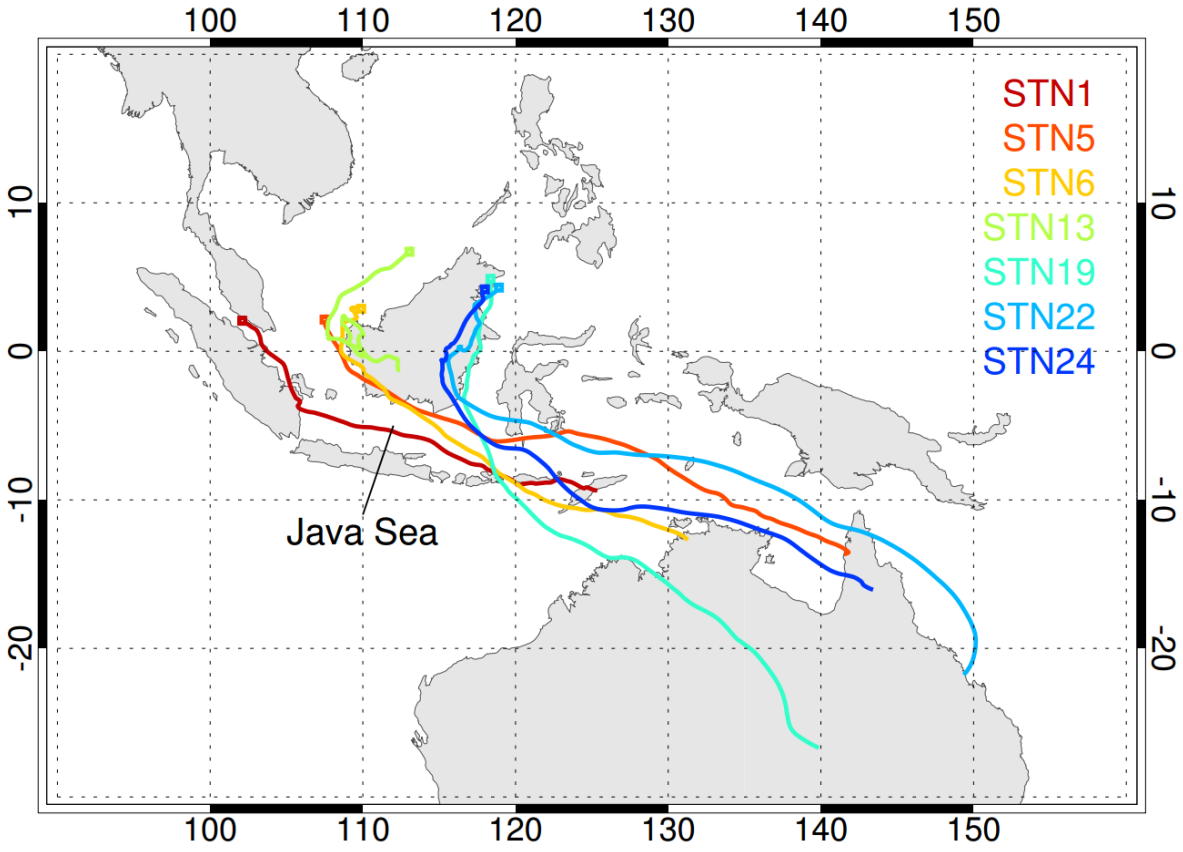

714

715 **Figure 3:** 10 days air distribution backward trajectories calculated from the NOAA
716 HYSPLIT model for selected stations.

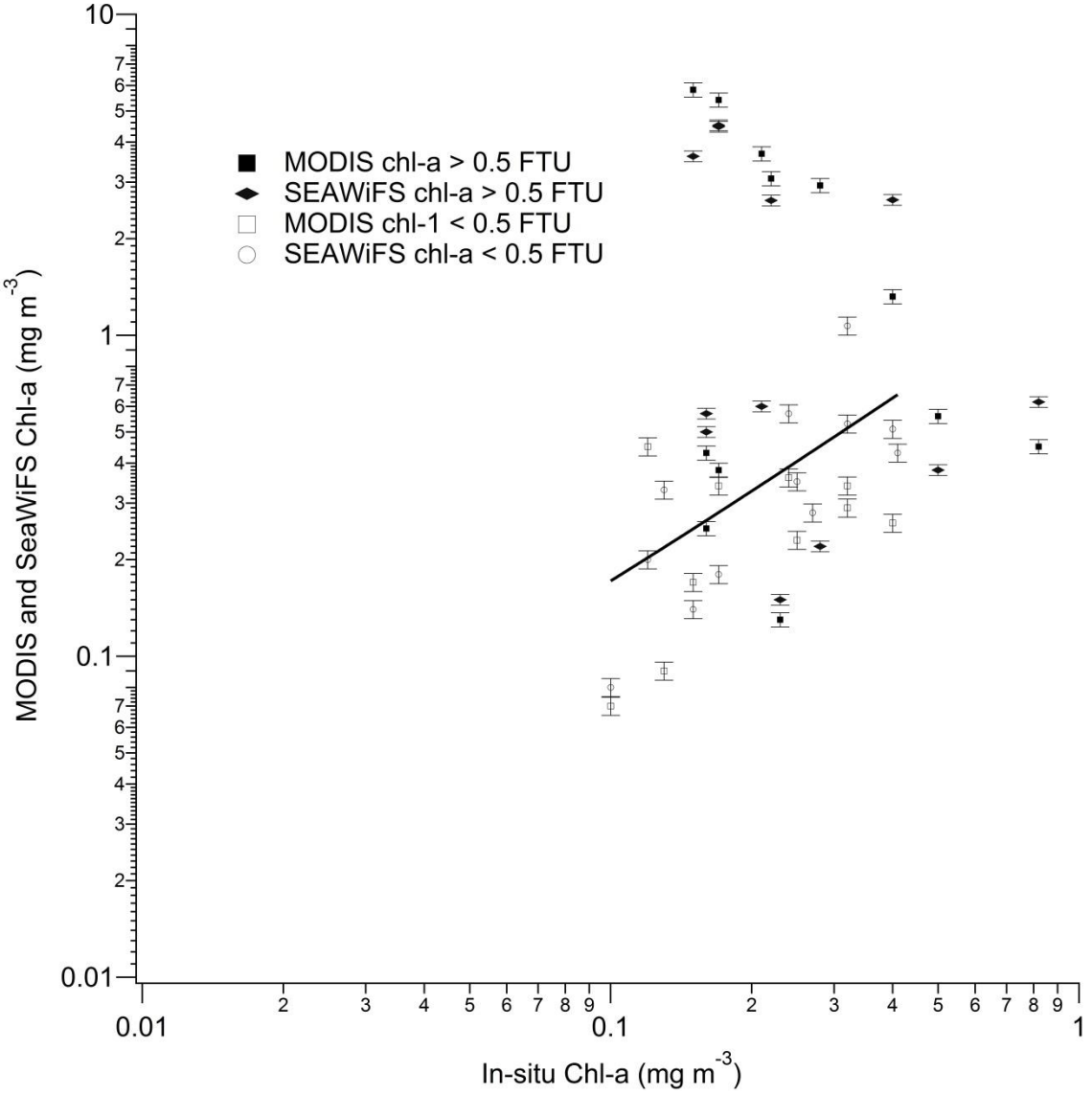

717

718 **Figure 4**: Chl-*a* concentration from the satellite data plotted against *in-situ* chl-*a*. The solid
719 symbols represent samples where turbidity was >0.5 FTU, and open symbols for turbidities
720 <0.5 FTU. The line is a linear fit to the lower turbidity samples.

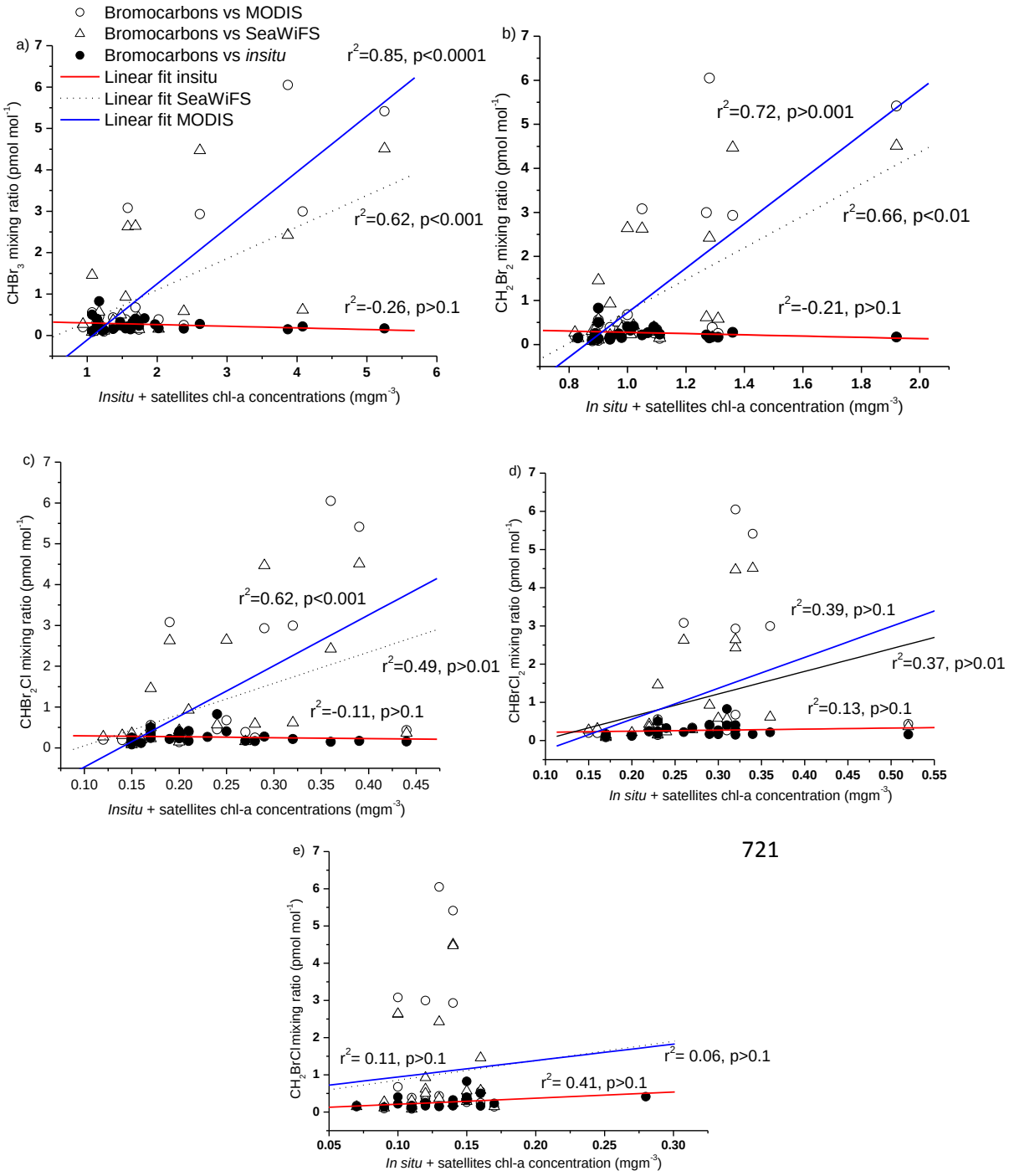

721

722

723

724

725

726

727

728 **Figure 5:** Monthly June-July 2009 VSLS bromocarbons mixing ratios a) $CHBr_3$, b) CH_2Br_2
729 c) $CHBr_2Cl$ d) $CHBrCl_2$ and e) CH_2BrCl as a function of *in situ* and satellite chl-*a*
730 concentration.

731

732

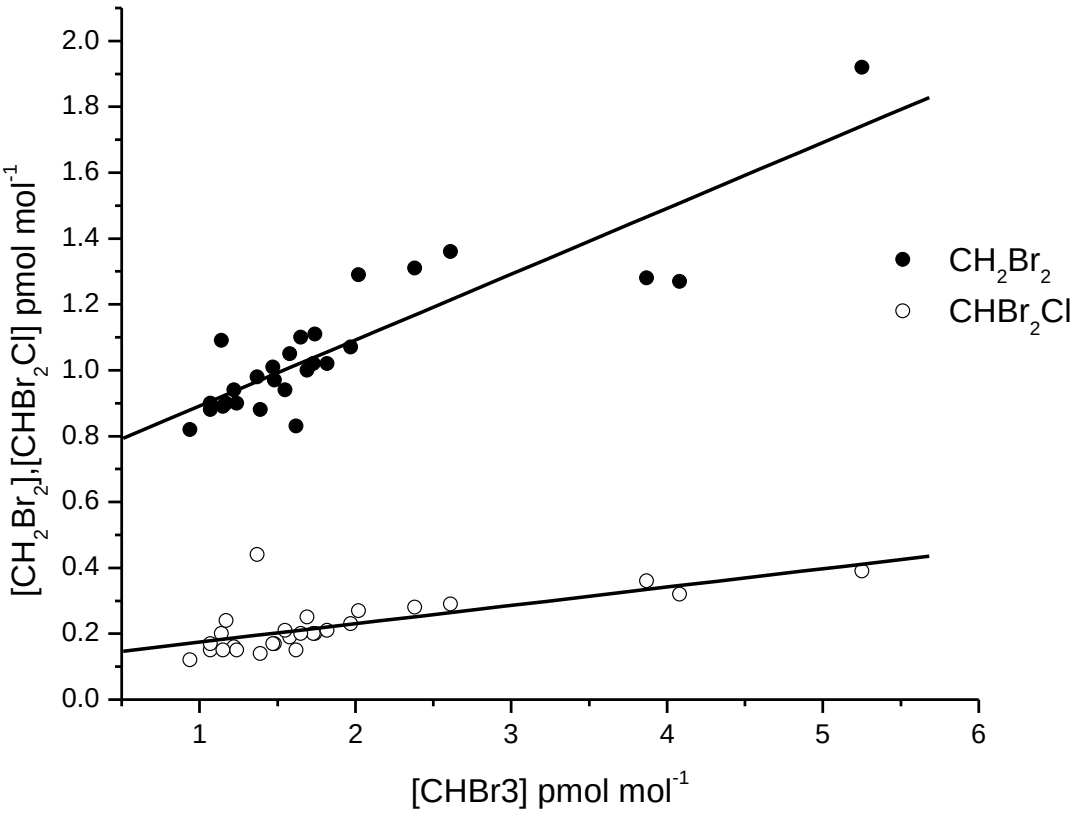

733

734 **Figure 6:** Plot for correlations of CH_2Br_2 and $CHBr_2Cl$ versus $CHBr_3$ concentrations.

735

736

737

738

739

a)

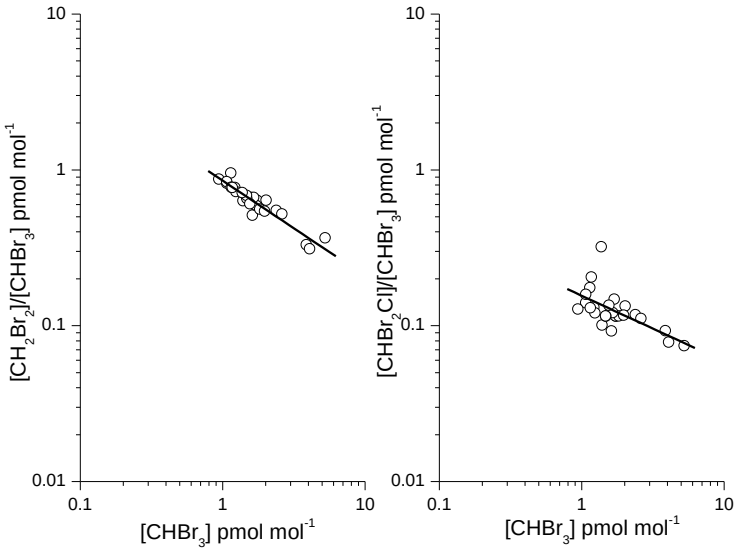

740

741 **b)**

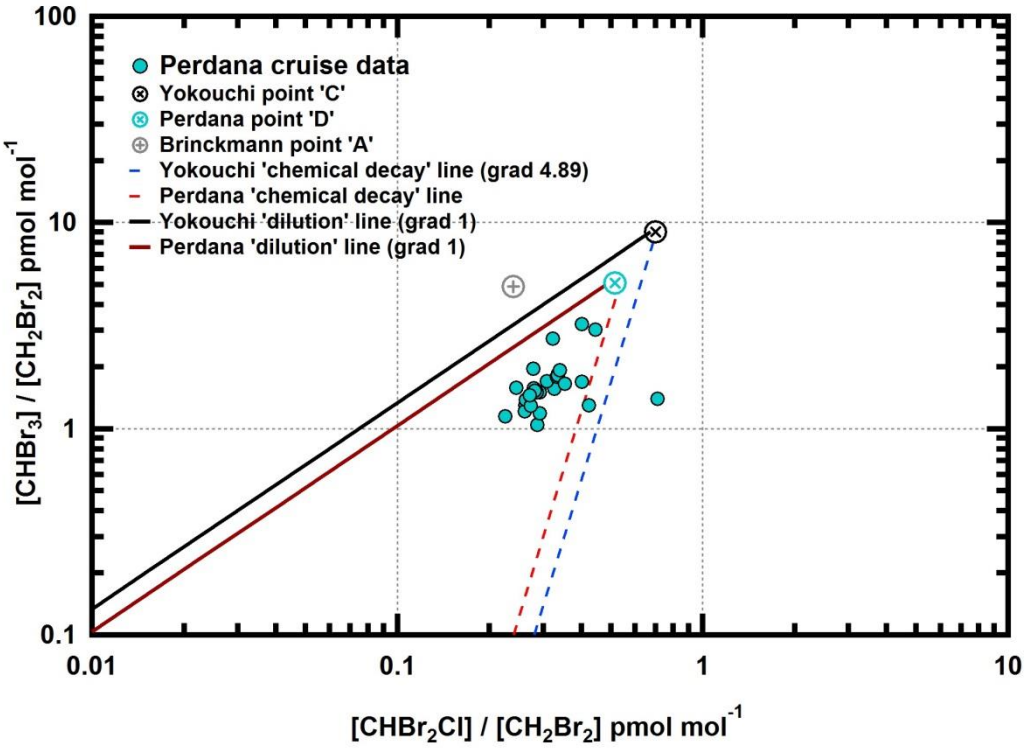

742

743 **Figure 7a) Log-log plot $CH_2Br_2/CHBr_3$ and $CHBr_2Cl/CHBr_3$ against $CHBr_3$ and 7b)**
744 Log-log plots of $CHBr_3/CH_2Br_2$ against $CHBr_2Cl/CH_2Br_2$ for all stations during Perdana
745 Cruise, following Yokouchi et al. (2005) and Brinckmann et al., (2011). The solid line is the
746 dilution line 1:1 and the solid dash line is the chemical decay line which estimated from the
747 lifetime of the 3 species in the atmosphere. In this case, we have followed the example of
748 Yokouchi et al. (2005) by using the lifetimes of 26 days ($CHBr_3$), 69 days ($CHBr_2Cl$) and 120
749 days (CH_2Br_2). Thus the decay line has a slope of 4.89. The black point at the top of the data

set is the point C in Yokouchi et al. (2005) and grey point is the point A in Brinckmann et al., (2011) log-log plots where $CHBr_3/CH_2Br_2$ to be around 9 and $CHBr_2Cl/CH_2Br_2$ to be around 0.7 from Yokouchi et al. (2005) and around 5 for $CHBr_3/CH_2Br_2$ and 0.2 for $CHBr_2Cl/CH_2Br_2$ from Brinckmann et al. (2011).

773 **Table 1:** Mean, standard deviation (in brackets) and range (in italics) values of the measured halocarbon concentrations in this work and values
774 from the literature based on tropical ocean areas (n.m. not mentioned).

			Bromocarbon's Mixing ratios						
Area	**Author**	**No. of samples**	**$CHBr_3$ Mean (std) *range***	**$CHBr_2Cl$ Mean (std) *range***	**CH_2Br_2 Mean (std) *range***	**$CHBrCl_2$ Mean (std) *range***	**CH_2BrCl Mean (std) *range***	***Chl-a* (mgm^{-3}) (std)**	**Turbidity (FTU)**
Strait of Malacca									
coastal	This study	4	3.69 (1.54) *1.85-5.25*	0.32(0.09) *0.19-0.39*	1.38(0.37) *1.05-1.92*	0.12 (0.02) *0.19-0.39*	0.12 (0.04) *0.1-0.14*	0.19(0.3)	3.33(1.22)
South China Sea									
Open ocean	This study	6	1.51 (0.4) *1.07-2.02*	0.21(0.05) 0.15-027	1.01(0.19) 0.88-1.29	0.22 (0.07) 0.17-0.32	0.10 (0.01) 0.09-0.11	0.17 (0.09)	0.19 (0.07)
coastal	This study	5	0.90(0.32) *0.82-1.02*	0.15(0.08) *0.12-0.2*	0.90(0.09) *0.82-1.02*	0.18(0.03) *0.15-0.22*	0.10(0.03) *0.07-0.15*	0.22(0.12)	0.15(0.07)
Sulu-Sulawesi seas									
coastal	This study	12	1.60(0.5) *1.07-2.61*	0.23(0.08) *0.15-0.44*	1.04(0.16) *0.89-1.36*	0.3(0.08) *0.22-0.52*	0.15(0.04) *0.12-0.28*	0.32(0.2)	1.54(0.92)
Previous studies in tropical regions									
South east Asia 100-105°E	Youkouchi et al., 1995		1.2 (n.m) *0.3-7.1*		0.77(n.m) *0.38-1.42*				
Western Pacific 43°N, 150°E & 4°N, 113°E	Quack & Suess., 1999		1.2(n.m) *0.38-10.67*	0.2(n.m) *0.07-1.34*		0.28(n.m) *0.08-2.96*			
San Cristobal Island (Loberia)	Yokouchi et al., 2005		14.2 (10.1) *4.2-43.6*	1.5(1.0) *0.5-4.1*	3.2(1.5) *1.8-7.6*				
Christmas Island (Topono)	Yokouchi et al., 2005		23.8 (10.7) *16.3-31.4*	2.0 (0.7) *1.5-2.4*	3.0 (1.0) *2.3-3.7*				
Java Island	Yokouchi et al., 2005		0.9 (0.4) *0.4-1.6*	0.2 (0.2) *0.1-0.6*	0.9 (0.2) *0.6-1.5*				
Pacific Equator	Yokouchi et al., 2005		1.9(0.9) *0.8-3.5*	0.3(0.1) *0.1-0.6*	1.3(0.5) *0.2-1.9*				

775